Characterization of the wrinkling limit curve using in-plane compression tests

MAGRINHO João P.G.[1,a] *, SANTOS João A.O.[1,b] and SILVA M. Beatriz[1,c]

[1]IDME, Instituto Superior Técnico, Universidade de Lisboa, 1049-001 Lisbon, Portugal

[a]joao.magrinho@tecnico.ulisboa.pt, [b]joao.oliveira.santos@tecnico.ulisboa.pt,
[c]beatriz.silva@tecnico.ulisboa.pt

Keywords: Wrinkling, Wrinkling Limit Curve (WLC), Onset of Wrinkling

Abstract. The global need for a green economy and the ongoing challenge of climate change have spurred demand for lightweight construction in various industries. This transition involves redesigning components with intricate geometries and advanced materials to reduce sheet metal thickness and the overall part weight. However, this pursuit of lightweight structures introduces challenges, particularly in wrinkling, raising the need to develop accurate methodologies for determining formability limits by wrinkling. This paper focuses on in-plane compression tests, specifically addressing the compression stress state associated with wrinkling in the flange area in deep drawing or a strip during flexible roll forming. Three physically-based methodologies (A, B, and C) are proposed to detect the onset of wrinkling and characterize the wrinkling limit curve (WLC) through experimental tests. Methodology A involves the analysis of the Z displacement, methodology B focuses on the in-plane minor strain rate evolution, and methodology C employs the analysis of the force-displacement evolution. The experimental work involves the mechanical characterization of AA1050-O aluminum sheets and the in-plane compression tests of rectangular specimens with different lengths. The results reveal distinct behaviors in wrinkling initiation for the different specimen lengths. The critical strain pairs obtained from each methodology are utilized to construct the WLCs in the principal strain space, providing insights into the formability limits by wrinkling.

Introduction

The transition to a green economy and the climate change challenge is fueling a trend toward lightweight construction in the transportation sector, i.e., automotive, aerospace, and aeronautical industries, general engineering, machine-tools, and architecture [1]. Redesigning parts with more complex geometries and new materials, with higher mechanical properties, allows the reduction of sheet metal thickness and the final weight of the parts. However, these factors make the material more prone to failure by wrinkling.

The methodologies for determining the onset and formability limits by wrinkling are not consolidated. The reason for this is attributed to the fact that wrinkling is influenced by a wide range of parameters that include the mechanical properties of the material, the geometry of the sheet part, the contact conditions imparted by the tools, and the applied level of stresses and strains [2].

The concept of the wrinkling-limit curve (WLC), which proposes the existence of a locus of in-plane strains defining the initiation of wrinkling in sheet metal forming, is credited to Havranek [3]. The precise position of the WLC typically occurs in the lower left-hand section of the second quadrant within the principal strain space, as schematically represented in Fig. 1. However, its specific location is often determined on a case-by-case basis, contingent upon the areas of focus within the sheet metal forming processes under analysis. Nevertheless, a minimal variation in the strain path can give rise to wrinkling in sheet metal forming [5], it is essential to conduct

experimental characterizations of WLCs under these representative loading conditions. This approach ensures that preventive measures can be implemented to avoid wrinkling.
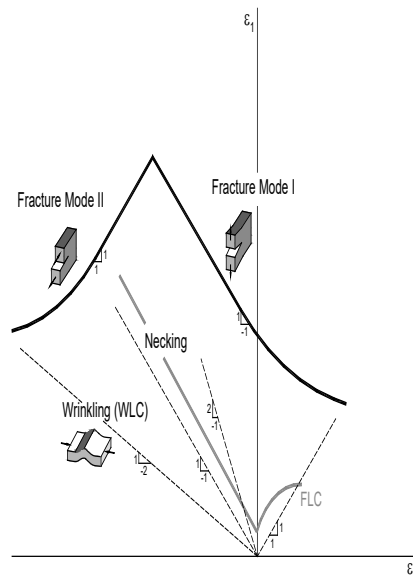

Fig. 1. Schematic representation of the formability limits by necking, fracture, and wrinkling in sheet metal forming [4].

Considering the compression state of stress directly related to the wrinkling of the flange area in a stamping operation or the compression stress state stems from the wrinkling registered in the flange area of a strip during flexible roll forming, this paper is focused on the in-plane compression test originally proposed by Kasaei et al. [6]. Three different methodologies to determine the onset of wrinkling and characterize the WLC are considered to evaluate their potential for successfully predicting the occurrence of wrinkling in sheet metal forming processes.

Experimentation

Mechanical Characterization. The investigation involved the mechanical characterization of commercially available AA1050-O aluminum sheets with 1.5 mm thickness. Tensile tests were conducted using an INSTRON 5900 universal testing machine, following the ASTM standard E8/E8M-16 [7], at room temperature. Test specimens were machined from the provided sheets at 0, 45, and 90º angles with respect to the rolling direction (RD) to characterize the anisotropy.

The mechanical properties obtained from the tensile tests are presented in Table 1, such as the modulus of elasticity, E, the yield stress, σ_Y, the ultimate tensile stress, σ_{UTS}, the elongation at break, A, and the planar anisotropy coefficient, r.

Table 1. Mechanical properties of aluminum AA1050-O sheet with 1.5 mm thickness [8].

Specimen Direction	Modulus of elasticity E (GPa)	Yield strength σ_Y (MPa)	Ultimate strength σ_{UTS} (MPa)	Elongation at break A (%)	Anisotropy coefficient r	K (MPa)	n
0º	78.63	24.78	72.74	45.98	1.08	136.94	0.27
45º	79.40	25.64	82.12	52.86	3.20	159.07	0.30
90º	78.36	24.11	71.48	47.26	0.81	134.44	0.27
Average	78.95	25.04	77.11	49.74	2.08	147.38	0.29

The average values included in Table 1 were determined as follows (where x denotes a mechanical property),
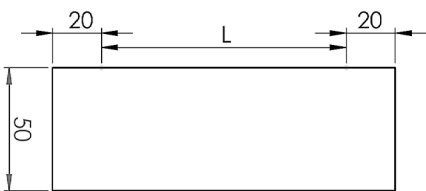
$$\bar{x} = \frac{x_0 + 2x_{45} + x_{90}}{4}. \tag{1}$$

The anisotropy coefficient derived from the tensile tests on sheets aligned at a 45º angle to the rolling direction exhibits a significantly greater value compared to sheets aligned at 0º and 90º. This phenomenon was previously recognized by Sharma et al. [9] in sheets resulting from the accumulative roll-bonding manufacturing process. The average stress-strain curve can be approximated by the following Ludwik-Hollomon's equation,

$$\bar{x} = 147.38 \, \bar{\varepsilon}^{0.29}. \tag{2}$$

Experimental Plane. Table 2 provides a summary of the in-plane compression tests employed for characterizing the WLC of the aluminum AA1050-O sheet. A minimum of five repetitions were conducted for each dimension among the four different lengths. The in-plane compression tests were executed under room temperature conditions and quasi-static operational settings, involving the monotonous application of a tensile load at a velocity of 5 mm/min. Specimens were cut from the supplied sheets perpendicular to the rolling direction of the sheet.

Table 2. Summary of the experimental work plan for the in-plane compression tests.

Geometry		Thickness t (mm)	Length L (mm)	Compression Specimen (CS)
		1.5	20	CS20
			35	CS35
			50	CS50
			100	CS100

The necessary testing equipment for the in-plane compression tests includes an Instron universal testing machine, model SATEC 1200 KN, and a double-action tool system (Fig. 2a), that converts the vertical displacement of the Instron punch to a horizontal displacement [2]. Additionally, these experimental tests also require the tool to fix the in-plane compression test specimen to the double-action tool (Fig. 2b). Steel shims were also used to ensure uniform pressure distribution when tightening and create different boundary conditions when intended.

Displacement and Strain Measurements. The determination of the onset of wrinkling in the aluminum sheet material of in-plane compression test specimens involved a three-dimensional measurement of displacement and strain on the sheet surface, conducted using a DIC system, the Dantec Dynamics Model Q-400 3D. The specimen surfaces were coated with a stochastic black speckle pattern against a uniformly matte white background. Illumination was provided by a single spotlight directed at the test specimens. The DIC system is equipped with two cameras boasting a 6-megapixel resolution, a 50.2 mm focal length, and an aperture of f/11 to enhance depth of focus. Image acquisition occurred at a frequency of 10 frames per second, and the correlation algorithm utilized the INSTRA 4D software (version 4.6, Dantec Dynamics, Skovlunde, Denmark). A facet size of 17 pixels, along with a spacing grid of 13 pixels, was employed in the analysis.

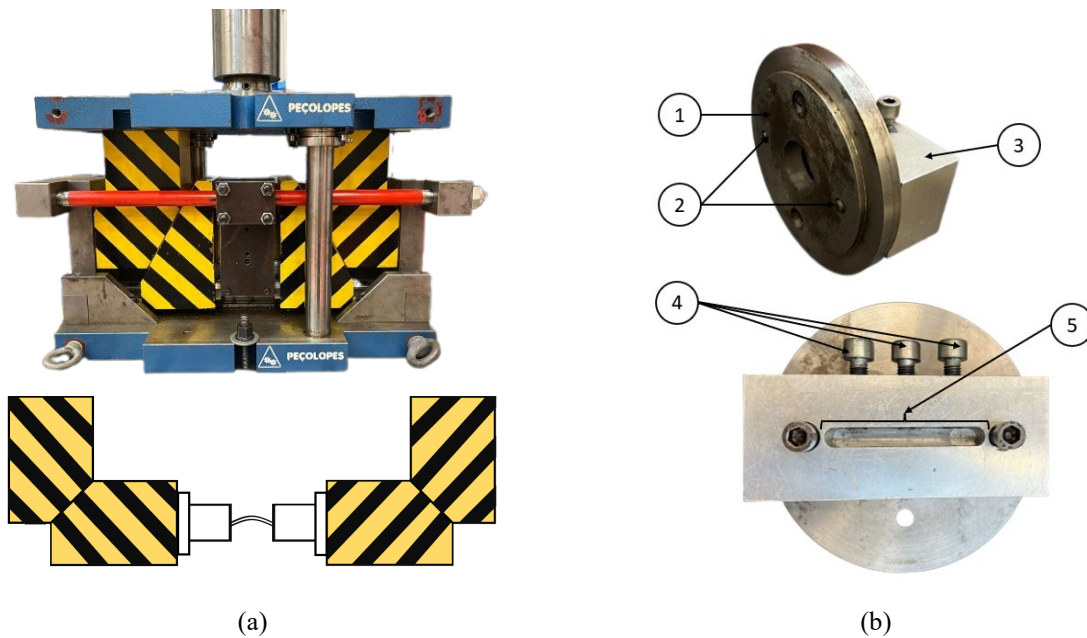(a)   (b)

Fig. 2. Photograph of (a) the double-action tool system [2] and (b) the tool to fix the in-plane compression test specimens: 1) die shoe; 2) fixation bolts; 3) sheet holder block; 4) sheet holder bolts; 5) sheet holder block slot.

Methodology

This paper proposes three physically-based methodologies to detect the onset of wrinkling and to determine the formability limits by wrinkling in sheet metal forming through experimental in-plane compression tests.

Methodology A. Methodology A relies on directly analyzing the Z displacement (perpendicular to the sheet surface) along the in-plane compression test specimen (section AA'), as depicted in Fig. 3a. The analysis of Z displacement along section AA' enables the determination of the amplitude of the plastic instability wave corresponding to the maximum Z displacement of section AA' (Fig. 3b). The schematic presentation of the evolution of the plastic instability wave over time along the in-plane compression test is illustrated in Fig. 3c. A critical amplitude of the plastic instability wave h_{crit} can be defined as 5-10% of the sheet thickness, as initially proposed by Du et al. [10] for Yoshida buckling tests.

The instant when the amplitude of the plastic instability wave equals the critical amplitude marks the point in time for determining the critical strain pairs along the strain loading path of a point localized in the central zone of section AA', as schematically shown in Fig. 3d. These critical strain pairs, obtained for in-plane compression test specimens with different dimensions, are then utilized to construct the WLC in the principal strain space.

Methodology B. Methodology B involves the direct analysis of the in-plane minor strain within the central zone of the in-plane compression test specimen, as depicted in Fig. 3a as the measuring area. This area, where strains are measured by the DIC system, corresponds to the zone with the maximum Z displacement of section AA'. Before the onset of instability, the evolution of the in-plane minor strain in the central zone of the in-plane compression test specimen is influenced by the specimen's geometry. However, after the occurrence of plastic instability, the direction of the evolution of in-plane minor strain changes. The analysis of the strain rate (the first-time derivative of in-plane minor strain) enables the detection of this phenomenon, and the minimum point corresponds to the critical time when buckling is initiated, as shown in Fig. 4a. The critical time signifies the moment when critical strain pairs can be determined from the strain loading path of a

point located in the central zone of section AA', as depicted in Fig. 4b. These critical strain pairs, obtained for in-plane compression test specimens with different geometries, are then utilized to construct the WLC in the principal strain space.
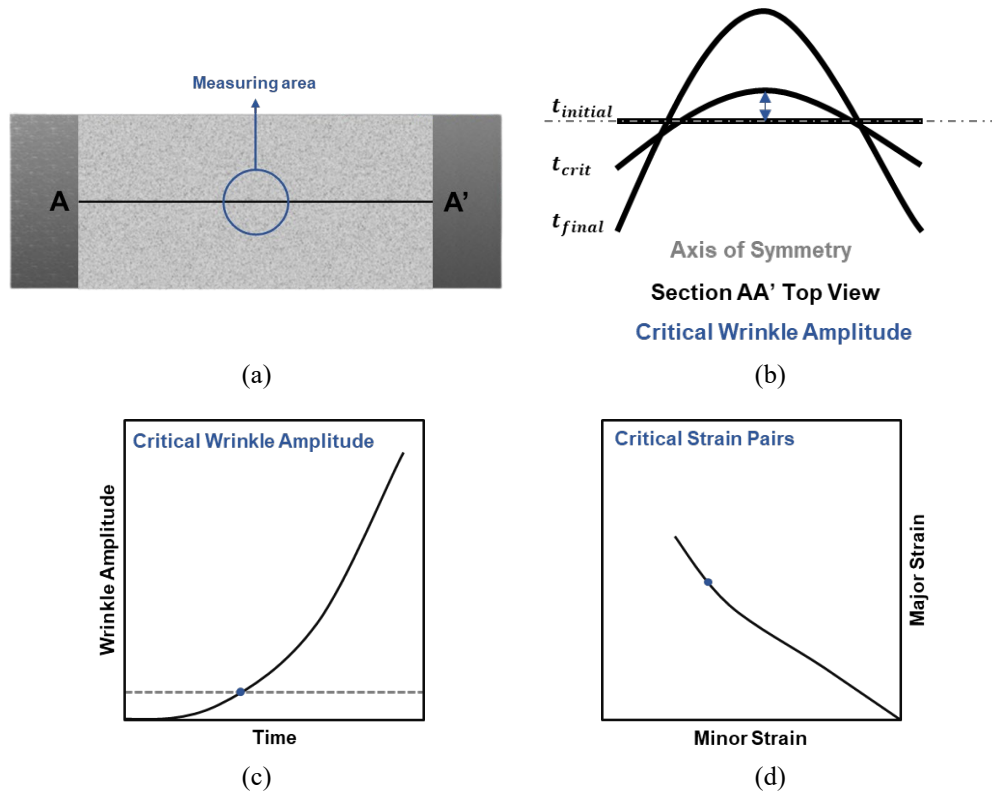

(a)

(b)

(c)

(d)

Fig. 3. Summary of methodology A: (a) schematic representation of the in-plane compression test; (b) identification of wrinkling amplitude; (c) evolution of the wrinkling amplitude over time; (d) representation of the strain loading path and identification of the critical strains in principal strain space.
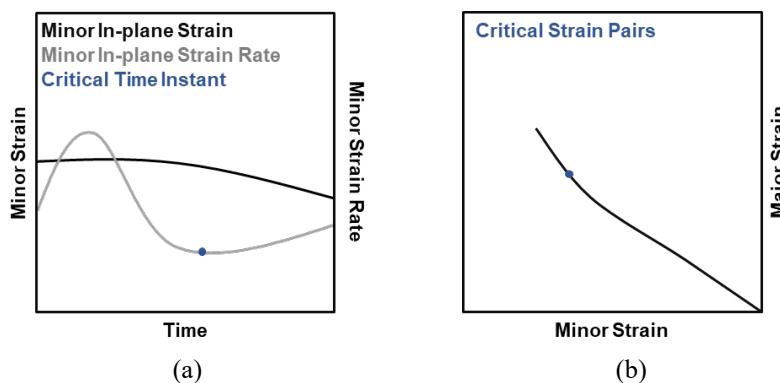

(a)

(b)

Fig. 4. Summary of methodology B: (a) evolution of the in-plane minor strain and strain rate; (b) representation of the strain loading path and identification of the critical strains in principal strain space.

Methodology C. Methodology C is based on the direct analyses of the force-displacement curves of the in-plane compression tests. The onset of wrinkling defined by this methodology occurs when a bifurcation point is reached in the force-displacement curve, as seen in Fig. 5a. The bifurcation

point occurs due to the existence of a secondary path E_S with lower deformation energy than in the primary path E_P, as explained by Kim and Yang [11]. The bifurcation point corresponds to the critical time and at this instant, the critical strain pairs can be determined from the strain loading path of a point located in the central zone of section AA', as depicted in Fig. 5b. These critical strain pairs, obtained for in-plane compression test specimens with different geometries, are then utilized to construct the WLC in the principal strain space.

$$W = \frac{E_P}{E_S} \geq 1$$

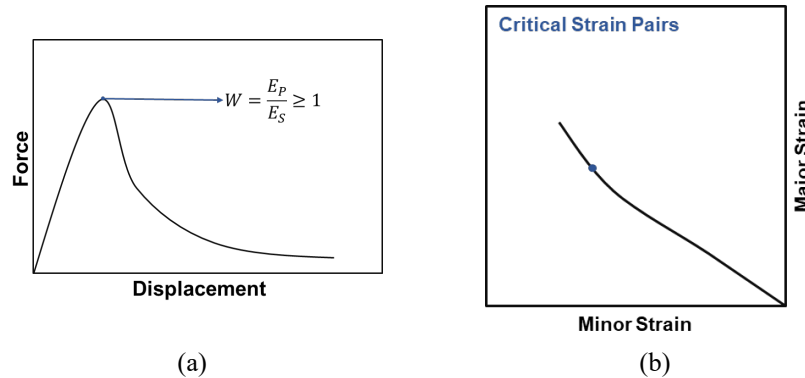(a)   (b)

Fig. 5. Summary of methodology C: (a) evolution of the forced displacement; (b) representation of the strain loading path and identification of the critical strains in principal strain space.

Results and Discussion

Methodology A. The position-dependent methodology defines the onset of wrinkling when the wrinkle amplitude is 5% of the sheet metal thickness. Since the thickness of the sheet metal is 1.5 mm, this means that the onset of wrinkling occurs when the wrinkle amplitude is 0.075 mm. This amplitude height is represented in Fig. 6a as the dashed-black line. Fig. 6a also presents the Z-displacement for the central point of each set of compression specimens, as represented in Fig. 6b. The rate at which the wrinkle amplitude increases is related to the increase in the length of the in-plane compression specimen, as is possible to verify the different rates of the wrinkle amplitude increase between the specimen with 20 mm and the specimen with 100 mm of length. The time difference between the onset of wrinkling defined by methodology A for the in-plane compression specimen with 20 and 100 mm of length is approximately 10s. Kasaei et al. [6] and Magrinho et al. [2] also registered that the onset of wrinkling occurs sooner for specimens with a higher length.

The critical instant corresponds to the instant of time that Z-displacement evolution intercepts the dashed-black line. For this instant, the critical strain pairs are determined to draw the WLC in the principal strain space.
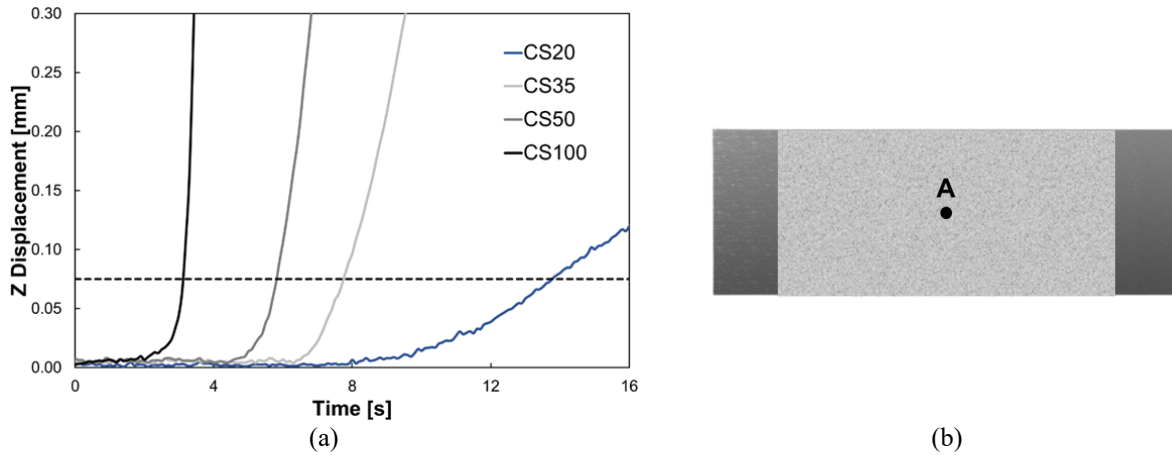
Fig. 6. (a) Z-displacement of the center of each set of in-plane compression test specimens with a length of 20, 35, 50, and 100 mm; (b) Point A located in the center of the in-plane compression specimen.

Methodology B. The physically-based methodology evaluates the in-plane minor strain rate evolution at the center of the in-plane compression test specimens, represented by the middle point along section AA' in Fig.s 7b and 7d. The in-plane minor strain and in-plane minor strain rate evolution over time at the center of test specimens with 20 and 100 mm of length are represented in Fig.s 7a and 7d, respectively.

By applying the same color scale to all specimens, it is possible to access the minor strain distribution on the surface of the in-plane compression test specimen. In Fig.s 7b and 7d it is possible to verify that there is a slight concentration of the in-plane minor strain in the direction perpendicular to the center of section AA'. Since all specimens wrinkled to the same side, away from the DIC system, the DIC cameras measured the bottom face of the wrinkle, which is the reason for the in-plane minor strain to have compressive values along the whole length of the specimen. The critical time instants for the onset of wrinkling defined by methodology B, show that when the length of the specimen increases, wrinkling occurs sooner. In addition, the critical in-plane minor strain continuously decreases as the length of the specimen increases. For this instant, the critical strain pairs are determined to draw the WLC in the principal strain space.

Methodology C. The onset of wrinkling determined by methodology C is defined by the bifurcation point, the maximum point, in the force-displacement curves presented in Fig. 8. The same procedure was also applied by Kasaei et al. [6] and Magrinho et al. [2] to determine the onset of wrinkling and the obtained results were similar. The force and displacement at which the bifurcation point occurs increases with the decrease in the specimen length.

Wrinkling Limit Curve. Fig. 9 represents the formability limits by wrinkling determined by in-plane compression tests in conjunction with the three different methodologies: A, B, and C. The WLCs were obtained by using the average critical strain pairs obtained from each methodology and imposing a polynomial regression of degree 2, which is the curve that best fits the behavior of the material in these experimental tests. Due to the difference in the average critical strain pairs obtained from methodology A when compared to those obtained from methodologies B and C, a 4x zoom is added to Fig. 9 to provide a more detailed view of the WLCs obtained from the latter methodologies.
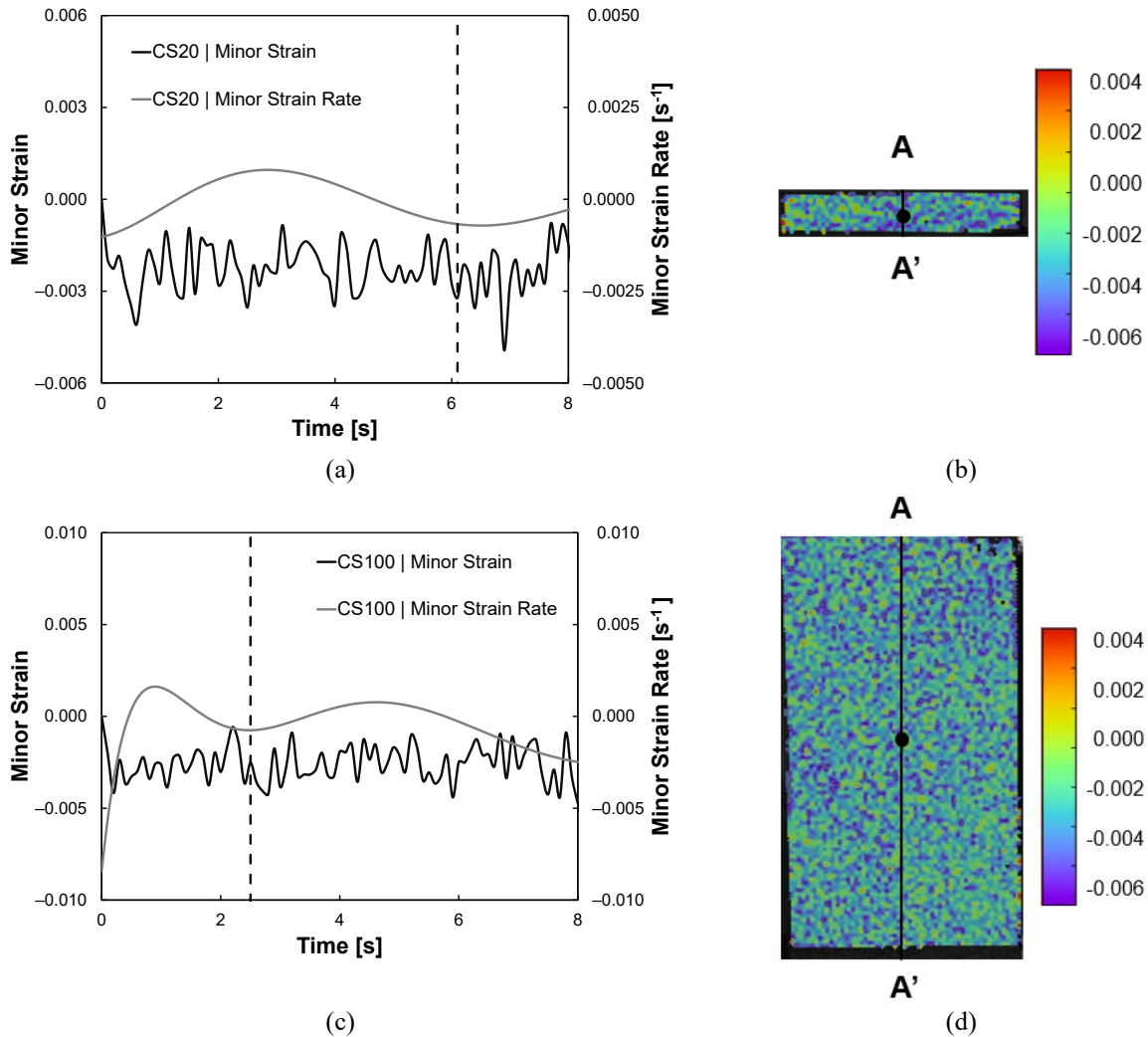
In-plane minor strain and in-plane minor strain rate evolution over time for specimens with lengths of (a) 20 and (c) 100 mm. In-plane minor strain rate distribution at the onset of wrinkling obtained from the DIC according to methodology B for specimens with lengths of (b) 20 and (d) 100 mm.

However, there is a common behavior in all specimens registered in all the methodologies, which corresponds to the following: the critical in-plane minor strain always increases in module with the decrease in the specimen length, while the in-plane major strain follows the same behavior except between the compression specimens with 35 and 20 mm of length, where it decreases. This behavior was also registered by Magrinho et al. [2] for aluminum alloy AA1050-O with thicknesses of 1, 2, 3, and 4 mm.

In Fig. 9 it is possible to verify that the ratio between in-plane minor and major strains for the critical strain pairs determined by methodology B and C for the specimens with a length of 100, 50, and 35 mm is approximately -1, while the specimens with a length of 20 mm have a $\beta = \varepsilon_2/\varepsilon_1 = -2$. For this reason, the WLC obtained from these methodologies initially has an approximate slope corresponding to pure shear and at the end tends to deviate towards the uniaxial compression deformation.
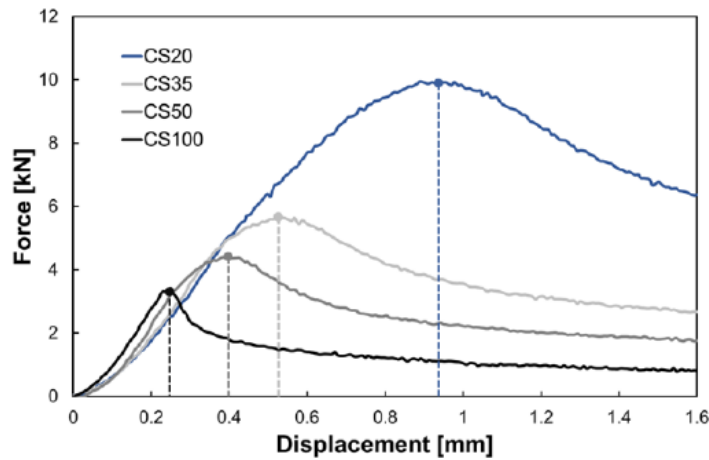
Fig. 8. Evolution of the force with displacement and identification of the bifurcation point for the in-plane compression test specimens with lengths of 20, 35, 50, and 100 mm.
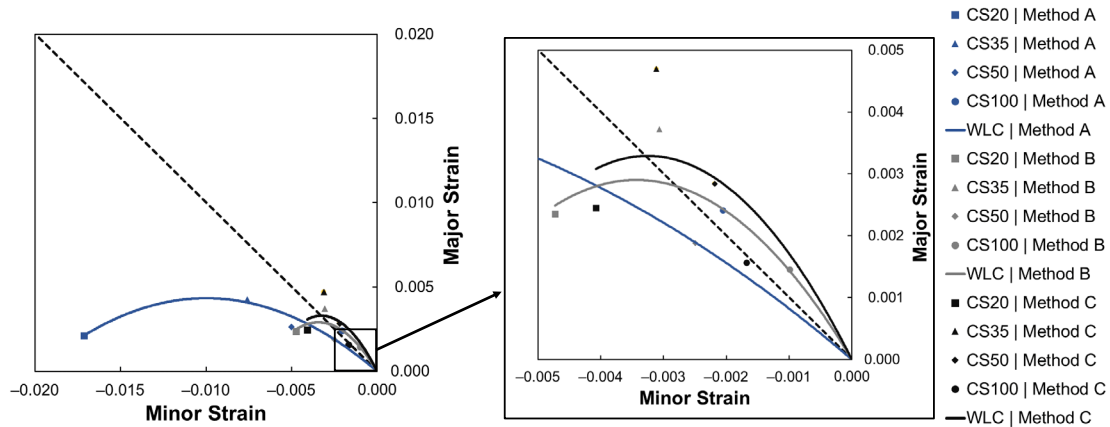

Fig. 9. Formability limits by wrinkling defined by methodology A, B, and C for AA1050-O aluminum sheet with 1.5 mm thickness.

In contrast, the critical strain pairs obtained from methodology A at the onset of wrinkling for the specimens with a length of 100 mm have an approximate ratio of -1. A $\beta = -2$ is obtained for the specimens with lengths of 50 and 35 mm. The in-plane strains ratio proceeds to decrease for the specimens with 20 mm length, reaching a value of $\beta = -8$. Hence, the WLC determined by methodology A continuously tends towards slopes of increasing compression state as the length of the specimen decreases.

Conclusions

In conclusion, this study introduces three robust methodologies (A, B, and C) for detecting the onset of wrinkling and characterizing the WLC in sheet metal forming processes. Through comprehensive experimental work, including mechanical characterization and in-plane compression tests on AA1050-O aluminum sheets with 1.5 mm thickness, the proposed methodologies exhibit their effectiveness in predicting wrinkling initiation under varying conditions.

Methodology A, focusing on Z displacement analysis, determines the onset of wrinkling by identifying the amplitude of the plastic instability wave. Methodology B, centered on in-plane minor strain rate evolution, utilizes DIC system measurements to detect critical times and strain pairs. Methodology C employs force-displacement curve analysis, identifying the bifurcation point to determine critical strain pairs.

The study highlights the influence of specimen length on wrinkling initiation, with distinct behaviors observed in the three methodologies. The obtained critical strain pairs contribute to constructing WLCs, offering valuable insights into formability limits by wrinkling. This research advances our understanding of wrinkling phenomena, aiding in developing preventive measures and design strategies for lightweight structures in various industries.

References

[1] M. Kleiner, M. Geiger, A. Klaus, Manufacturing of Lightweight Components by Metal Forming. CIRP Annals 52(2) (2003) 521–542. https://doi.org/10.1016/S0007-8506(07)60202-9

[2] J.P.G. Magrinho, C.M.A. Silva, M.B. Silva, P.A.F. Martins, Formability limits by wrinkling in sheet metal forming, Proceedings of the Institution of Mechanical Engineers, Part L: Journal of Materials: Design and Applications 232(8) (2016) 681–692. https://doi.org/10.1177/1464420716642794

[3] J. Havranek, Wrinkling limit of tapered pressing, Journal of the Australian Institute of Metals 20 (1975) 114–119.

[4] P.A.F. Martins, N. Bay, A.E. Tekkaya, A.G. Atkins, Characterization of fracture loci in metal forming. International Journal of Mechanical Sciences 83 (2014) 112–123. https://doi.org/10.1016/j.ijmecsci.2014.04.003

[5] A.M. Szacinski, P.F. Thompson, Investigation of the existence of a wrinkling-limit curve in plastically deforming metal sheet, Journal of Materials Processing Technology 25(2) (1991) 125-137. https://doi.org/10.1016/0924-0136(91)90085-S

[6] M.M. Kasaei, H. Moslemi Naeini, G.H. Liaghat, C.M.A. Silva, M.B. Silva, P.A.F. Martins, Revisiting the wrinkling limits in flexible roll forming, The Journal of Strain Analysis for Engineering Design 50(7) (2015) 528-541. https://doi.org/10.1177/0309324715590956

[7] ASTM Standard E8/E8M, Standard Test Methods for Tension Testing of Metallic Materials, West Conshohocken, USA: ASTM International. 2016. https://doi.org/10.1520/E0008_E0008M-16A

[8] J.A.O. Santos, J.P.G. Magrinho, M.B. Silva, Physically-Based Methodology for the Characterization of Wrinkling Limit Curve Validated by Yoshida Tests, Metals 13(4) (2023) 746. https://doi.org/10.3390/met13040746

[9] S. Sharma, R.P. Singh, S. Kumar, Mechanical Anisotropy of Aluminium AA1050 and Aluminium Alloy AA6016 produced by Accumulative Roll Bonding, International Journal of Innovations Engineering and Technology 7 (2016) 350–356.

[10] B. Du, J. Xie, H. Li, C. Zhao, X. Zhang, X. Yuan, Determining factors affecting sheet metal plastic wrinkling in response to nonuniform tension using wrinkling limit diagrams, Thin-Walled Structures 147 (2020) 106535. https://doi.org/10.1016/j.tws.2019.106535

[11] J.B. Kim, D.Y. Yang, Prediction of wrinkling initiation in sheet metal forming processes, Engineering Computations 20(1) (2003) 6–39. https://doi.org/10.1108/02644400310458810